

## Simulations of Rising Hydrodynamic and Magnetohydrodynamic Bubbles

P. M. Ricker,<sup>1,2</sup> K. Robinson,<sup>3</sup> L. J. Dursi,<sup>3,4</sup> R. Rosner,<sup>3,4,5</sup> A. C. Calder,<sup>3,4</sup> M. Zingale,<sup>6</sup>  
J. W. Truran,<sup>3,4</sup> T. Linde,<sup>3,4</sup> A. Caceres,<sup>3,5</sup> B. Fryxell,<sup>3,4</sup> K. Olson,<sup>7</sup> K. Riley,<sup>3</sup> A. Siegel,<sup>3</sup> and  
N. Vladimirova<sup>3</sup>

<sup>1</sup> *Dept. of Astronomy, University of Illinois at Urbana-Champaign, Urbana, IL 61801*

<sup>2</sup> *National Center for Supercomputing Applications, Urbana, IL 61801*

<sup>3</sup> *Center for Astrophysical Thermonuclear Flashes, The University of Chicago, Chicago, IL 60637*

<sup>4</sup> *Dept. of Astronomy & Astrophysics, The University of Chicago, Chicago, IL 60637*

<sup>5</sup> *Dept. of Physics, The University of Chicago, Chicago, IL 60637*

<sup>6</sup> *Dept. of Astronomy & Astrophysics, The University of California, Santa Cruz, Santa Cruz, CA 95064*

<sup>7</sup> *UMBC/GEST Center, NASA/GSFC, Greenbelt, MD 20771*

Motivated by recent *Chandra* and *XMM-Newton* observations of X-ray emission voids in galaxy cluster cooling flows, we have investigated the behavior of rising bubbles in stratified atmospheres using the FLASH adaptive-mesh simulation code. We present results from two-dimensional simulations with and without the effects of magnetic fields, and with varying bubble sizes and background stratifications. We find purely hydrodynamic bubbles to be unstable; a dynamically important magnetic field is required to maintain a bubble's integrity. This suggests that, even absent thermal conduction, for bubbles to be persistent enough to be regularly observed, they must be supported in large part by magnetic fields. We also observe that magnetically supported bubbles leave a tail as they rise. The structure of these tails may provide clues to the bubble's dynamical history.

### 1. Introduction

Recent high-resolution X-ray observations by the *Chandra* and *XMM-Newton* satellites have dramatically challenged the standard picture of multiphase cooling flows in clusters of galaxies (Böhringer et al. 2002). First, no evidence from spatially resolved spectroscopy has been observed for the presence of gas colder than about 1–2 keV (e.g. Schmidt et al. 2001; Peterson et al. 2001; Kaastra et al. 2001; Tamura et al. 2001; Matsushita et al. 2002). Second, high-resolution imaging has provided evidence for large-scale motions that can heat the intracluster medium (e.g. McNamara et al. 2000, 2001; Forman et al. 2002; Blanton et al. 2003). It has long been known that many of the same clusters that harbor cooling flows also contain large central galaxies with active nuclei. However, the extent to which these active galactic nuclei (AGN) influence the dynamical state of the cooling ICM has only become apparent through the new X-ray observations. These observations show that AGN are associated with massive outflows of magnetized plasma that displace the cooling gas. The ‘bubbles’ thus produced are known to be magnetized because radio observations show regions of synchrotron emission coinciding with the regions of low X-ray emission, and the polarization of this radiation shows Faraday rotation effects consistent with dynamically important magnetic fields (e.g. Allen et al. 2001; Nulsen et al. 2002). The emerging picture is that bubbles represent the late stages of propagation of the magnetized, relativistic jets produced by AGN into the ICM, after they have slowed

and reached approximate pressure equilibrium with the ICM (Reynolds et al. 2002).

The influence of these magnetized bubbles on the cooling ICM is still poorly understood. How efficiently does the bubble plasma mix with the ICM? Does it heat the cooling flow sufficiently to avoid the formation of multiphase gas and the possible formation of stars? If so, how — by radiative heating, magnetic reconnection, or some other process? What fraction of the total energy budget of a cluster is contributed by magnetic fields and cosmic rays? Could these active regions be sites for the acceleration of the ultra-high-energy cosmic rays seen in some air-shower experiments?

Owing to the geometrical and physical complexity of the AGN-cooling flow environment, numerical simulations are the best theoretical tools available for addressing these questions. While bubbles in liquids are well-studied (e.g. Magnaudet & Eames 2000; Harper 1972), bubbles in cluster cooling flows should differ from bubbles in liquids in several important ways. In particular, molecular forces present in liquids (e.g., surface tension, viscosity) will not play a significant role, and magnetic fields may be important. These differences should affect the dynamics and stability properties of bubbles.

In this paper we describe simulations of rising hydrodynamic and magnetohydrodynamic bubbles that we have performed using the adaptive mesh refinement (AMR) hydrodynamics code FLASH (Fryxell et al. 2000). We investigate the relative importance of geometry, stratification, density contrast, and thermal and magnetic pres-

sure on the stability of bubbles. Complete details of this work are given by Robinson et al. (2003); here we confine ourselves to a brief overview of our methods and some of our results.

## 2. Initial models and methods

Our initial model is an underdense circular bubble in an isothermal, stratified atmosphere with an imposed constant gravitational acceleration in the  $y$ -direction. An ideal equation of state is used, with a ratio of specific heats  $\gamma = 5/3$ . The sound speed is chosen, through the temperature and mean molecular weight, so that our standard simulation domain spans approximately three pressure scale heights. For most of our simulations, we simulate two-dimensional boxes in planar geometry. We vary the stratification by varying the gravitational acceleration. We also vary the size of the bubble.

We performed several simulations in which the density contrast between the bubble and the background is caused by a higher temperature in the bubble in horizontal pressure equilibrium with its surroundings. We also performed simulations in which part of the pressure support for the underdense bubble comes from an azimuthal magnetic field. In the former case, we performed simulations with and without a background magnetic field. The bubble is in horizontal pressure equilibrium at every point inside the bubble; since the bubbles considered here are significant fractions of a pressure scale height, the bubble's pressure structure is itself somewhat stratified.

In all of our simulations the physics is scale-free; for comparison with real clusters we have scaled our results as follows. The density  $\rho_0$  and the pressure  $p_0$  at the base of the grid are  $4.0 \times 10^{-26} \text{ g cm}^{-3}$  and  $4.2 \times 10^{-11} \text{ dyn cm}^{-2}$ , respectively, corresponding to an ambient temperature of 0.70 keV. The computational box spans  $120 \times 150 \text{ kpc}$ , and our fiducial initial bubble radius is 9 kpc. The gravitational acceleration,  $g = 7.0 \times 10^{-9} \text{ cm s}^{-2}$ , corresponds roughly to the value one might expect from a  $10^{14} M_\odot$  cluster at a radius of 20 kpc, assuming a Navarro, Frenk, & White (1997) total density profile and typical values for the central gas density ( $10^{-3} \text{ cm}^{-3}$ ) and total gas fraction (0.15).

We perform our simulations using the FLASH code (Fryxell et al. 2000). FLASH is an adaptive-mesh reactive hydrodynamics code that includes both hydrodynamic and magnetohydrodynamic (MHD) solvers. FLASH's main hydrodynamic solver, based on the piecewise parabolic method (PPM; Colella & Woodward 1984), has undergone a rigorous validation and verification process (Calder et al. 2002). The method we use for our MHD calculations is described in Powell et al. (1999). The two solvers use similar techniques, but the MHD solver uses lower-order polynomial reconstruction than the PPM solver. We use the techniques described in Zingale et al. (2002) to maintain hydrostatic equilibrium. The simulations described here were performed with a maximum effective grid size of  $512 \times 640$ , refining the mesh where the second derivative of the pressure or density is large. Our boundary conditions are reflecting on the left and right and hydrostatic at the top and

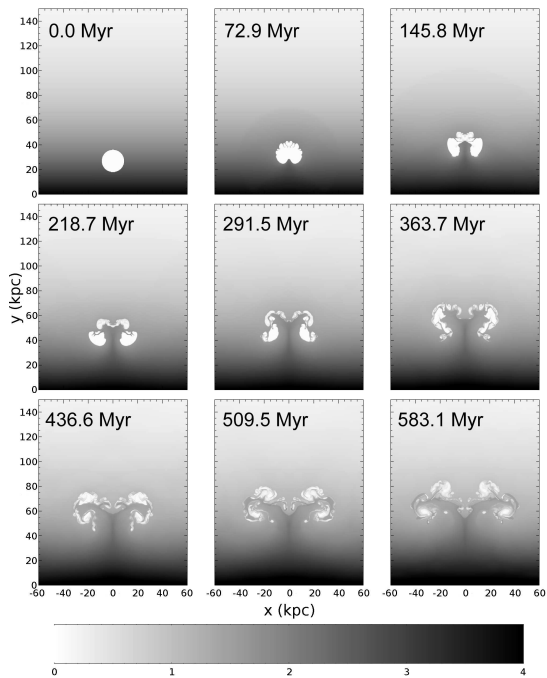


FIG. 1.— Density evolution in the fiducial hydrodynamic case.

bottom. In MHD simulations, the magnetic boundary conditions are reflecting on the left and right and zero-gradient at the top and bottom.

We neglect radiative cooling and thermal conduction; this approximation is discussed in more detail by Robinson et al. (2003).

## 3. Results

### 3.1. Hydrodynamic Bubbles

Our fiducial case consists of a purely hydrodynamic bubble with the ambient parameter values discussed in the previous section. The density inside the bubble is  $0.01\rho_0$ , the bubble's radius is 9 kpc, and the geometry is Cartesian. The evolution of the gas density for this case is shown in Figure 1.

In the absence of magnetic effects, nothing prevents the complete disruption of the bubble. The bubble's rise itself generates vortical motion in the surrounding fluid on the same scales as the bubble and with velocities similar to the rise velocity of the bubble. These motions contribute to the disruption of bubbles on timescales of order the bubble rise time,  $t_R = \sqrt{4R/g}$ , where  $R$  is the bubble radius. For our fiducial case,  $t_R \approx 130 \text{ Myr}$ . At the top the bubble is also susceptible to the growth of the Rayleigh-Taylor instability on scales smaller than  $R$ . The sides of the bubble exhibit shear instability as the bubble rises.

Increasing the bubble interior density to  $0.1\rho_0$  does not significantly affect the late-time dynamics of the bubble. One way of understanding this is that in both cases, the bubble densities are very much less than the surrounding environment, so that it is the momentum of the fluid in the environment, not the bubble, which dominates

the dynamics. Quantitatively, the Atwood number,  $A \equiv (\rho_> - \rho_<)/(\rho_< + \rho_>)$ , is 0.82 in the 10:1 case, and 0.98 in the 100:1 case — so while the bubble density changes by a factor of 10, the Atwood number, which controls both the buoyant force and the evolution of the Rayleigh-Taylor instability, changes only by 20%.

Increasing the bubble radius to 15 kpc increases the wavenumber range of the Rayleigh-Taylor-unstable region and increases the role of this instability relative to the induced vortical motions in the ambient medium.

### 3.2. MHD Bubbles

For MHD bubbles we fixed the bubble interior density at  $0.1\rho_0$  to avoid numerical problems resulting from a large jump in Alfvén speed across the edge of the bubble. We considered pressure-supported bubbles in several different background magnetic field configurations as well as magnetically supported bubbles in vertical background fields. We discuss the latter case below.

For magnetically supported bubbles we assume a force-free magnetic field  $\mathbf{B}$  everywhere in the domain except at the boundary between the bubble and the ambient medium, where the Lorentz force balances the jump in gas pressure. Inside the bubble we use the “flux rope” solution of Cargill & Chen (1996):

$$B_\theta = \begin{cases} B_b \frac{r}{R} & r \leq R \\ 0 & r > R \end{cases} \quad (1)$$

$$B_z = \begin{cases} B_b \sqrt{4 - 2 \left(\frac{r}{R}\right)^2} & r \leq R \\ B_{z0} & r > R \end{cases} \quad (2)$$

$$B_b = \sqrt{\frac{8\pi}{3} p_0 \left(1 - \frac{\rho_b}{\rho_0}\right) + B_{z0}^2} \quad (3)$$

Here  $\rho_b$  is the bubble interior density and  $B_{z0}$  is the ambient magnetic field (aligned with the  $z$ -axis).

In this case the bubble maintains its form as it rises (Figure 2). The bubble eventually overshoots the height of neutral buoyancy, decelerates, then falls back again. As it rises, the bubble entrains a wake of ambient material and also develops a dense shell. Similar shells have been noted in *Chandra* observations of bubbles. The shell appears to be “grabbed” by the azimuthal field at time  $t = 0$  when the entire bubble is surrounded by higher density material. The shell’s density does not change significantly as the bubble rises, suggesting that the bubble simply advects ambient material.

## 4. Conclusions

We find that bubbles without supporting magnetic fields are torn apart by instabilities and vortical motions before they can move an entire bubble height. This is surprising, as ‘ghost’ bubbles — not radio bright, and thus presumably no longer powered — are observed (Mazzotta et al. 2002; Fabian et al. 2000; McNamara et al. 2000) at a significant distance in bubble radii away from the radio source which presumably formed them. The existence of these bubbles can be explained if they are supported by an internal magnetic field.

This work also suggests that the shells of brighter material surrounding these bubbles may be caused by magnetic diffusion of the field that maintains them. There

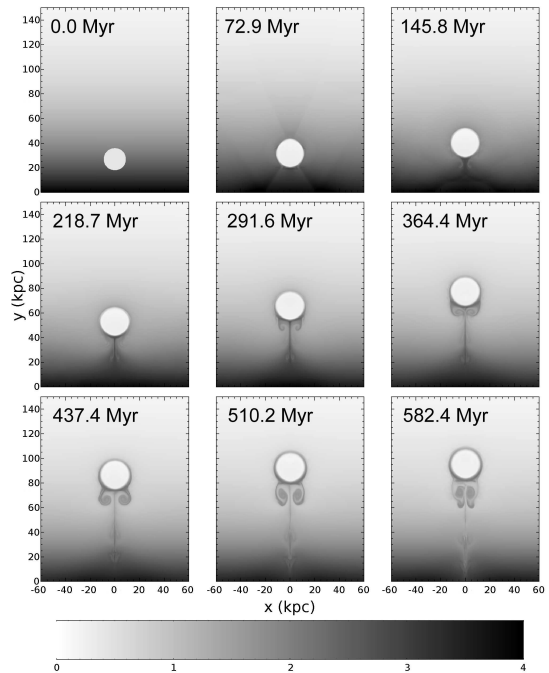


FIG. 2.— Density evolution in the magnetically supported bubble case.

is also numerical evidence suggesting a wake left behind the bubble as it moves. The appearance of such wakes in cluster radio maps would be a good indicator of the past motion of these bubbles.

Since magnetic fields may be necessary to keep bubbles intact as they travel, our future work will focus on MHD simulations, and in particular simulations with more realistic geometries. Thermally supported bubbles in MHD simulations generalize easily to 3D, but magnetically supported bubbles will be more complicated, since no analytic solutions are known for the 3D spherical analog to the “flux rope” solution we have used. However, such a field, numerically generated, should also be able to support the bubble without disruption. Including the divergent geometry appropriate to the center of a cluster will also be a necessary step.

Support for this work was provided by DOE grant number B341495 to the ASCI Alliances Center for Astrophysical Thermonuclear Flashes at the University of Chicago. PMR is supported by the University of Illinois and the National Center for Supercomputing Applications (NCSA). K. Robinson was supported by the NSF REU program at the University of Chicago. LJD is supported by the Krell Institute CSGF. MZ is supported by DOE SciDAC grant DE-FC02-01ER41176 to the Supernova Science Center at UCSC.

## References

- Allen, S. W., Taylor, G. B., Nulsen, P. E. J., Johnstone, R. M., David, L. P., Ettori, S., Fabian, A. C., Forman, W., Jones, C., & McNamara, B. 2001, *MNRAS*, 324, 842
- Blanton, E. L., Sarazin, C. L., & McNamara, B. R. 2003, *ApJ*, 585, 227
- Böhringer, H., Matsushita, K., Churazov, E., Ikebe, Y., & Chen, Y. 2002, *A&A*, 382, 804
- Calder, A. C., Fryxell, B., Plewa, T., Rosner, R., Dursi, L. J., Weirs, V. G., T., D., Robey, H. F., Kane, J. O., Remington, B. A., Drake, R. P., Dimonte, G., Zingale, M., Timmes, F. X., Olson, K., Ricker, P., MacNeice, P., & Tufo, H. M. 2002, *ApJS*, 143, 201
- Cargill, P. J. & Chen, J. 1996, *Journal of Geophysical Research*, 101, 4855
- Colella, P. & Woodward, P. 1984, *JCP*, 54, 174
- Fabian, A. C., Sanders, J. S., Ettori, S., Taylor, G. B., Allen, S. W., Crawford, C. S., Iwasawa, K., Johnstone, R. M., & Ogle, P. M. 2000, *MNRAS*, 318, L65
- Forman, W., Jones, C., Markevitch, M., Vikhlinin, A., & Churazov, E. 2002, in *Lighthouses of the Universe: The Most Luminous Celestial Objects and Their Use for Cosmology Proceedings of the MPA/ESO*, 51
- Fryxell, B., Olson, K., Ricker, P., Timmes, F. X., Zingale, M., Lamb, D. Q., MacNeice, P., Rosner, R., Truran, J. W., & Tufo, H. 2000, *ApJS*, 131, 273
- Harper, J. F. 1972, *Adv. Appl. Mech.*, 12, 59
- Kaastra, J. S., Ferrigno, C., Tamura, T., Paerels, F. B. S., Peterson, J. R., & Mittaz, J. P. D. 2001, *A&A*, 365, L99
- Magnaudet, J. & Eames, I. 2000, *Ann. Rev. Fluid Mech.*, 32, 659
- Matsushita, K., Belsole, E., Finoguenov, A., & Böhringer, H. 2002, *A&A*, 386, 77
- Mazzotta, P., Kaastra, J. S., Paerels, F. B., Ferrigno, C., Colafrancesco, S., Mewe, R., & Forman, W. R. 2002, *ApJ*, 567, L37
- McNamara, B. R., Wise, M., Nulsen, P. E. J., David, L. P., Sarazin, C. L., Bautz, M., Markevitch, M., Vikhlinin, A., Forman, W. R., Jones, C., & Harris, D. E. 2000, *ApJ*, 534, L135
- McNamara, B. R., Wise, M. W., Nulsen, P. E. J., David, L. P., Carilli, C. L., Sarazin, C. L., O'Dea, C. P., Houck, J., Donahue, M., Baum, S., Voit, M., O'Connell, R. W., & Koekemoer, A. 2001, *ApJ*, 562, L149
- Navarro, J. F., Frenk, C. S., & White, S. D. M. 1997, *ApJ*, 490, 493
- Nulsen, P. E. J., David, L. P., McNamara, B. R., Jones, C., Forman, W. R., & Wise, M. 2002, *ApJ*, 568, 163
- Peterson, J. R., Paerels, F. B. S., Kaastra, J. S., Arnaud, M., Reiprich, T. H., Fabian, A. C., Mushotzky, R. F., Jernigan, J. G., & Sakelliou, I. 2001, *A&A*, 365, L104
- Powell, K. G., Roe, P. L., Linde, T. J., Gombosi, T. I., & De Zeeuw, D. L. 1999, *J. Comp. Phys.*, 154, 284
- Reynolds, C. S., Heinz, S., & Begelman, M. C. 2002, *MNRAS*, 332, 271
- Robinson, K., Dursi, L. J., Ricker, P. M., Rosner, R., Calder, A. C., Zingale, M., Truran, J. W., Linde, T., Caceres, A., Fryxell, B., Olson, K., Riley, K., Siegel, A., & Vladimirova, N. 2003, *ApJ*, accepted
- Schmidt, R., Allen, S. W., & Fabian, A. C. 2001, *MNRAS*, 327, 1057
- Tamura, T., Kaastra, J. S., Peterson, J. R., Paerels, F. B. S., Mittaz, J. P. D., Trudolyubov, S. P., Stewart, G., Fabian, A. C., Mushotzky, R. F., Lumb, D. H., & Ikebe, Y. 2001, *A&A*, 365, L87
- Zingale, M., Dursi, L. J., Zuhone, J., Calder, A. C., Fryxell, B., Plewa, T., Truran, J. W., Caceres, A., Olson, K., Ricker, P. M., Riley, K., Rosner, R., Siegel, A., Timmes, F. X., & Vladimirova, N. 2002, *ApJS*, 143, 539